DOI:10.1021/jf102326m

JOURNAL OF AGRICULTURAL AND FOOD CHEMISTRY
ARTICLE

# Ultrasensitive Electrochemical Immunoassay of Staphylococcal Enterotoxin B in Food Using Enzyme-Nanosilica-Doped Carbon Nanotubes for Signal Amplification

Dianping Tang,* Juan Tang, Biling Su, and Guonan Chen

Key Laboratory of Analysis and Detection for Food Safety (Ministry of Education and Fujian Province), Department of Chemistry, Fuzhou University, Fuzhou 350108, China

A new sandwich-type electrochemical immunoassay for ultrasensitive detection of staphylococcal enterotoxin B (SEB) in food was developed using horseradish peroxidase-nanosilica-doped multiwalled carbon nanotubes (HRPSiCNTs) for signal amplification. Rabbit polyclonal *anti*-SEB antibodies immobilized on the screen-printed carbon electrode (SPCE) and covalently bound to the HRPSiCNTs were used as capture antibodies and detection antibodies, respectively. In the presence of SEB analyte, the sandwich-type immunocomplex could be formed between the immobilized *anti*-SEB on the SPCE and *anti*-SEB-labeled HRPSiCNTs, and the carried HRP could catalyze the electrochemical reduction of $H_2O_2$ with the help of thionine. The high content of HRP in the HRPSiCNTs could greatly amplify the electrochemical signal. Under optimal conditions, the reduction current increased with the increase of SEB in the sample, and exhibited a dynamic range of 0.05−15 ng/mL with a low detection limit (LOD) of 10 pg/mL SEB (at $3\sigma$). Intra- and interassay coefficients of variation were below 10%. In addition, the assay was evaluated with SEB spiked samples including watermelon juice, soymilk, apple juice, and pork food, receiving excellent correlation with results from commercially available enzyme-linked immunosorbent assay (ELISA).

**KEYWORDS: Staphylococcal enterotoxin B; food; immunoassay; electrochemical immunosensor**

## INTRODUCTION

The analysis of foods to assess the presence of both biological (pathogenic bacteria) and chemical contaminants is a practice of crucial importance for ensuring food safety and quality (*1*, *2*). Conventional bacterial testing methods rely on specific microbiological media to isolate and enumerate viable bacterial cells in food (*3*), while the majority of chemical contaminants are commonly analyzed using separation techniques coupled to various detectors such as gas chromatography-flame ionization detector (*4*), gas chromatography−mass spectrometry (*5*), gas chromatography-electronic capture detector (*6*), high performance liquid chromatography−ultraviolet rays (*7*), high performance liquid chromatography-fluorescence detection (*8*), high performance liquid chromatography−mass spectrometry (*9*), and surface-enhanced Raman scattering (*10*). Despite many advances in this field, it is still a challenge to explore new approaches and strategies for the improvement of detection sensitivity in low-concentration food analysis (*11*−*14*).

Electrochemical immunoassays and immunosensors, based on the antigen−antibody interaction, have recently attracted considerable interest because of their high sensitivity, low cost, and inherent miniaturization (*15*−*17*). To achieve a high sensitivity, different labeled methods and technologies have been employed for the signal amplification of antigen−antibody interaction, such as metal nanoparticles (nanogold and nanosilver) (*18*), semiconductor nanoparticles (*19*), enzyme-loaded carbon nanotubes (*20*), and electroactive component-loaded nanovehicles (silica nanoparticle, polymer beads, and liposome beads) (*21*−*24*). The Ju group reported a highly sensitive electrochemical immunosensor for detection of microcytin-LR with a LOD of 30 pg/mL using functionalized single-walled carbon nanohorns as trace labels (*18*). Pividori and his colleagues designed a rapid and sensitive electrochemical magneto genosensing for determination of food pathogenic bacteria using the double-tagged amplicon (*25*). The highlight of this method is to directly monitor the concentration of *Salmonella sp*. at a LOD of 1.0 CFU/mL without any pretreatment. Moreover, the LOD could further decrease to 0.04 CFU/mL if the sample was preenriched for 6 h. The enormous signal enhancement associated with the use of nanomaterial labels and the formation of nanomaterial−antibody−antigen assemblies provided the basis for ultrasensitive electrochemical detection of food-related contaminants.

For the successful development of electrochemical immunoassays, signal amplification and noise reduction are very crucial for obtaining low detection limits. Carbon nanotubes (CNTs) with high surface area-to-weight ratio, excellent mechanical properties, and fast electron-transfer capabilities have been extensively

*Author to whom correspondence should be addressed. E-mail: dianping.tang@fzu.edu.cn. Fax: +86 591 2286 6135. Phone: +86 591 2286 6125.

 Published on Web 09/28/2010 

explored in electroanalytical chemistry (*26*−*28*). However, CNTs were usually employed as an immobilized material for the fabrication of biosensors/immunosensors. Recently, the Jiang group (*29*) and the Ju group (*18*) investigated the applications using functional CNTs as labels for ultrasensitive electrochemical immunoassays. The nanolabels were easily prepared by noncovalent modification or covalent conjugation with antibodies. Moreover, the Wang group also demonstrated that a CNT with 1 μm length could conjugate about 9,600 enzyme molecules (*30*). In these methods, the biomolecules were usually immobilized on the surface of CNTs, however. It is practicable that bioactive enzyme molecules are doped into the CNTs. As so, the functionalized CNTs inside and outside the CNTs contain hundreds to thousands of enzyme molecules. Using the functional CNTs as labels, the electrochemical signal might be enhanced.

Staphylococcal enterotoxin B (SEB) is an exotoxin produced by *Staphylococcus aureus* (*31*). It is one of the toxins responsible for staphylococcal food poisoning in humans and has been produced by some countries as a biological weapon (*32*). Thus, there is a need for the development of validated analytical methods for rapid and cost-effective screening of SEB on a large scale and at low concentration levels. Currently, a wide range of methods are available, ranging from liquid chromatography coupled to mass spectrometry to rapid methods based on immunological principles (*33*−*35*). It is predicted that techniques involving novel nanoparticle labels may become one of the main trends in the near future. To the best of our knowledge, there is no report focusing on the electrochemical immunoassay of SEB in food using enzyme and nanosilica-doped carbon nanotubes for signal amplification of electrochemical immunoassay. Herein, we synthesized a horseradish peroxidase-nanosilica-functionalized multiwalled carbon nanotube (HRPSiCNT) to label *anti*-SEB antibodies, which were used as detection antibodies for ultrasensitive electrochemical immunoassay of SEB in food on the *anti*-SEB/nanogold/thionine-coating screen-printed carbon electrode (SPCE). With sandwich-type immunoassay format, the formed immunocomplex was measured relative to the $H_2O_2$−PBS system with a thionine-mediated electron transfer process. The reduction current increased with the increment of SEB in the sample. The aim of this work is to exploit an advanced nanomaterial label for ultrasensitive electrochemical detection of low-concentration biocompounds in food.

## MATERIALS AND METHODS

**Materials and Chemicals.** Rabbit polyclonal *anti*-staphylococcal enterotoxin B antibody (*anti*-SEB, fractionated antiserum, lyophilized powder), staphylococcal enterotoxin B from *Staphylococcus aureus* (SEB, ≤0.25% staphylococcal enterotoxin A), thionine acetate salt (dye content ∼90%), bovine serum albumin (BSA, lyophilized powder, ∼66 kDa) and horseradish peroxidase (HRP, essentially salt free, lyophilized, ∼100 units/mg, EC: 1.11.1.7) were purchased from Sigma-Aldrich (St. Louis, MO). 10 nm gold colloids were synthesized according to our previous protocol (*36*). Multiwalled carbon nanotubes (CNTs, CVD method, purity ≥98%, diameter 60−100 nm, and length 1−2 μm) were supplied by Shenzhen Nanoport Co. Ltd. (Shenzhen, China). Tetramethoxysilane (TEOS), *N*-(3-dimethylaminopropyl)-*N*′-ethylcarbodiimide hydrochloride (EDC), and *N*-hydroxysulfosuccinimide sodium salt (NHS) were obtained from Sigma-Aldrich. Cyclohexane, *n*-hexanol, and ammonium hydroxide (25%, w/w) were purchased from Merck (Darmstadt, Germany). All other reagents were of analytical grade and were used without further purification. Ultrapure water obtained from a Millipore water purification system (≥18 MΩ, Milli-Q, Millipore) was used in all assays. 0.1 M acetic acid buffered saline (ABS, pH 5.5) was prepared by mixing the stock solutions of NaAc and HAc, and 0.1 M KCl was added as the supporting electrolyte. A buffer solution (PBS) of 0.1 M $NaH_2PO_4$ containing 0.1 M KCl was prepared, and the pH (pH 3.5−8.5) was adjusted with additional $Na_2HPO_4$ solution.

**Synthesis of HRP-Nanosilica-Doped CNTs (HRPSiCNTs).** Prior to experiment, the shortened carboxylate CNTs were prepared as follows (*18*): The multiwalled carbon nanotubes were initially sonicated in a mixture solution containing $H_2SO_4$ and $HNO_3$ (3:1, v/v) for 4 h, and then the mixture was filtered and washed repeatedly with water until pH was about 7.0. During this process, the long CNTs were shortened, the metallic and carbonaceous impurities were removed, and carboxylate groups were generated on the CNT surface (*18*).

Next, the shortened carboxylate CNTs were used for the preparation of HRPSiCNTs at room temperature (RT) using a reverse micelle method as follows: (i) A mixture was prepared by adding 5.0 g of Triton X-100, 4.0 mL of *n*-hexanol and 1.0 g of the shortened carboxylate CNTs into 20 mL of cyclohexane solution, and vigorously stirred 18 min; (ii) 1.0 mL of HRP (100 mg/mL) and 3.0 mL TEOS were injected into the mixture, and continuously stirred 30 min; (iii) 5.0 mL of $NH_3 \cdot H_2O$ (25%, w/w) was dropped into the stirring mixture, and vigorously stirred for 24 h; and (iv) 5.0 mL of acetone was added, and the mixture was washed with ethanol and water, and filtered using vacuum-filter method with nitrocellulose membrane (pore size, 0.2 μm). The synthesized HRPSiCNTs were collected on the membrane, which were used for the conjugation of *anti*-SEB antibodies.

**Preparation of *Anti*-SEB-HRPSiCNTs Bioconjugates.** *Anti*-SEB antibodies were conjugated onto the surface of the shortened carboxylate HRPSiCNTs consulting to the literature (*37*−*39*). In detail, 0.2 g of HRPSiCNTs was added into 5 mL of 0.1 M 2-(*N*-morpholino)-ethanesulfonic acid buffer (pH 6.0) containing 0.4 M EDC and 0.1 M NHS, and sonicated for 30 min. The mixture was centrifuged for 10 min at 14,000 rpm. The obtained HRPSiCNTs were dispensed into 5 mL of pH 8.0 PBS, and 300 μL of 0.1 mg/mL *anti*-SEB (as detection antibodies) was injected. The resulting mixture was slightly stirred at 150 rpm for 12 h at 4 °C, followed by centrifugation for 5 min at 4,000 rpm to remove the nonreacted antibodies. After contrifugation, the obtained bioconjugates were incubated with 2.5% (w/w) BSA for 1 h at RT to block the unreacted and nonspecific sites. Finally, the as-prepared nanoprobes (denoted as *anti*-SEB-HRPSiCNTs) were stored in pH 7.4 PBS with a finite concentration of 40 mg/mL at 4 °C when not in use. For comparison, another two nanoprobes were prepared and used in this study including HRP-labeled *anti*-SEB (HRP-*anti*-SEB) and *anti*-SEB-labeled multiwalled carbon nanotubes (*anti*-SEB-CNTs). The prepared process of *anti*-SEB-HRPSiCNTs is schematically illustrated in **Scheme 1a**.

**Preparation of Electrochemical Immunosensor.** The electrochemical immunosensor was prepared on a screen-printed carbon electrode (SPCE), which contained a graphite working electrode (2 mm in diameter), an Ag/AgCl reference electrode and a graphite auxiliary electrode. The insulating layer printed around the working area constituted an electrochemical microcell using a semiautomatic screen-printing machine (Baccini and Dek 1202) with a 156 thread/in. polyester screen, a stainless steel flood blade, and a polyurethane squeegee (Weymouth, U.K.) according to our previous report (*40*). Initially, a layer of electropolymerized thionine film was deposited onto the surface of the SPCE using scanning for 20 cycles between −1.5 V and +1.5 V at 50 mV/s in 0.1 M thionine−PBS. Following that, the thionine-modified electrode was placed into 10 nm gold colloids, and treated for 12 h at 4 °C. Subsequently, the obtained SPCE was submerged into 0.1 mg/mL *anti*-SEB solution (as capture antibodies), and incubated for 12 h at 4 °C. The formed immunosensor (denoted as *anti*-SEB/nanogold/thionine/SPCE) was incubated in 100 mg/mL BSA−PBS for 60 min at RT to eliminate nonspecific binding effect and block the remaining active groups. The finished immunosensor was stored at 4 °C when not in use.

**SEB Electrochemical Assays.** Electrochemical measurements were carried out with a CHI 430A Electrochemical Workstation (Chenhua, Shanghai, China) on the as-prepared SPCE. The electrochemical measurement of SEB levels mainly consisted of the following steps: (i) 20 μL of SEB standard solution or real samples with various concentrations was dropped to the SPCE surface, and incubated for 18 min at RT to form the antigen−antibody complex; (ii) after washing with pH 7.4 PBS, 20 μL of *anti*-SEB-HRPSiCNTs (40 mg/mL) was added into the detection cell, and incubated for another 18 min at RT to construct a sandwich-type immunocomplex; and (iii) 50 μL of pH 5.5 ABS buffer containing 8.0 mM $H_2O_2$ was injected into the cell, and differential pulse voltammetry (DPV) from −400 to 0 mV (vs Ag/AgCl) with a pulse amplitude of 50 mV and a

**Scheme 1.** (**a**) Preparation and Functionalization of HRPSiCNTs and (**b**) Multisignal Amplification and Comparison of the Sandwich-Type Electrochemical Immunoassay with Various Immunoassay Protocols

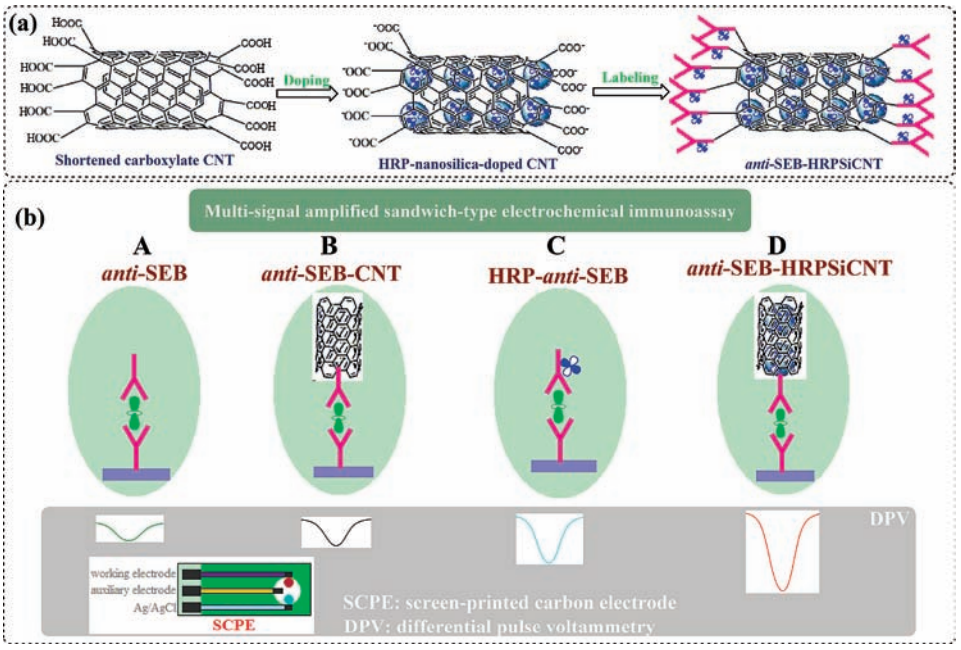


pulse width of 50 ms was collected and registered as the sensor signals. Analyses are always made in triplicate. The measurement protocol is shown **Scheme 1b**.

**Food Samples and Elution Procedure.** *Calibration Curve*. Fresh milk matrix for further addition calibration was prepared as follows: 1 mL of fresh milk sample (fat percentage: 3.25%) was initially diluted into 9 mL of water, and then SEB standards with various volumes were spiking into the milk matrix. The milk samples were assayed using the electrochemical immunoassay after incubation with matrix-toxin for 18 min.

*Food Sample Spiking*. To spike a sample of natural 100% watermelon juice, soymilk, and natural 100% apple juice, 15 mL of sample was initially transferred directly into a centrifuge tube, and then the sample was centrifuged for 20 min at 14,000 rpm. The resulting suspension was transferred into a fresh tube at a finite volume of 15 mL with water. For the pork food, 3.75 g of sample was initially placed in a centrifuge tube, then 15 mL of methanol/water (80:20, v/v) was added, and then the mixtures were sonicated for 60 s to assist extraction. Following that, these samples were centrifuged for 20 min at 14,000 rpm. Finally, 3 mL of the suspension was collected and transferred into another centrifuge tube and diluted to 15 mL with water. The real samples were prepared by spiking aliquots of SEB standards into different volumes of extraction. These spiking food samples were monitored using the electrochemical immunoassay and commercially available ELISA.

**ELISA Analysis.** Wells of microtiter plates (Haimen, Jiangsu, China) were initially coated by adding 0.1 mL of SEB−BSA ($1 \times 10^{-3}$ mg/mL) and incubating overnight at 4 °C, and then incubated with 0.3 mL of BSA (2 mg/mL) for 30 min at 37 °C. After the plate was washed 3 times with PBS, 0.1 mL of sample mixture ($1 \times 10^{-3}$ mg/mL *anti*-SEB in 2 mg/mL BSA−PBS, 1:1 with sample) was added to each well and incubated for 30 min at 37 °C. Following that, 0.1 mL of alkaline phosphatase (AP)-*anti*-mouse IgG (Sigma) was added to each well and incubated for 30 min at 37 °C. Finally, 0.1 mL of substrate Bluephos (Haimen) was added to each well, and the plate was monitored for 30 min at 620 nm by an Anthos 2001 reader (Anthos Mikrosysteme GmbH, Krefeld, Germany).

## RESULTS AND DISCUSSION

**Characteristics of HRPSiCNTs and Bioconjugates.** In this contribution, the long multiwalled carbon nanotubes were initially shortened and functionalized with carboxylate groups. Using the water-in-oil (W/O) microemulsion system, the water-soluble CNTs can be mixed with the HRP and TEOS aqueous solution, and the HRP and TEOS can diffuse inside the CNTs. With the help of ammonium hydroxide, the HRP-doped silica nanoparticles could be grown inside the CNTs. To verify the successful synthesis of the HRPSiCNTs, various characterization methods were used. First, we used scanning electron microscope (SEM, a Hitachi S-3000N, Japan) to investigate the CNT surface before and after modification with HRP and nanosilica particles. **Figure 1a** shows the SEM image of the shortened carboxylated CNTs, which displayed a homogeneous surface and good dispersion. When HRP-doped silica nanolayer was attached to the multiwalled carbon nanotubes, a rough surface appeared (**Figure 1b**). At the same time, the silica nanolayer could be faintly observed on the CNTs.

Could HRP and silica be really encapsulated into the hollow CNTs? $N_2$ adsorption isotherms of CNTs and HRPSiCNTs were investigated, and the results are displayed in **Figure 1c**. As indicated in **Figure 1c**, type IV adsorption isotherm and an H1 hysteresis loop are observed for porous material. In the range of 0.7−1.0 Pa, steplike curves were due to capillary condensation taking place in porous material. When HRP and silica were attached into the hollow CNTs, BET surface area (BET: Brunauer, Emmet, Teller, $m^2/g$) was obviously increased. The reason might be the fact that HRP-doped silica nanoparticles were formed inside the hollow CNTs, and increased the specific surface area.

Furthermore, the interaction between the CNTs and proteins could be demonstrated with UV−vis absorption spectrometry (Hitachi Instrument, Japan). A 398 nm of absorption peak was observed at HRP molecules according to our previous report (*24*). When HRP and silica were doped into the CNTs, the peak at 398 nm could be also achieved for HRPSiCNTs. The result suggested that the absorption peak of the doped HRP was not changed, and maintained its native characteristic. When the synthesized HRPSiCNTs were conjugated with *anti*-SEB antibodies, two absorption peaks at 398 and 278 nm were obtained (**Figure 1d**). On the basis of the results mentioned above, we might make a conclusion that the HRPSiCNTs could be formed and biofunctionalized using the reverse micelle method and EDC−NHS conjugate technique.

**Electrochemical Characteristics. Figure 2** displays the cyclic voltammograms of variously modified electrodes at 50 mV/s in

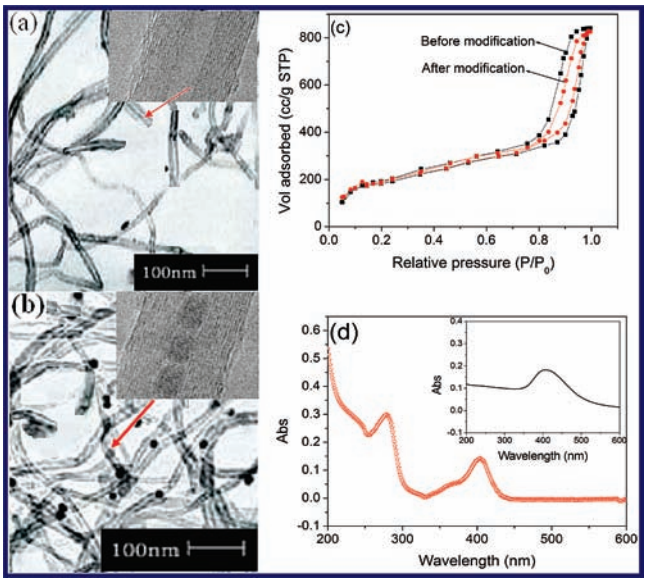


**Figure 1.** SEM images of (**a**) CNTs and (**b**) HRPSiCNTs, (**c**) $N_2$ adsorption−desorption isotherms at 77 K for CNTs and HRPSiCNTs, and (**d**) UV−vis absorption spectroscopy of *anti*-SEB-HRPSiCNTs (inset: UV−vis absorption spectroscopy of HRPSiCNTs).

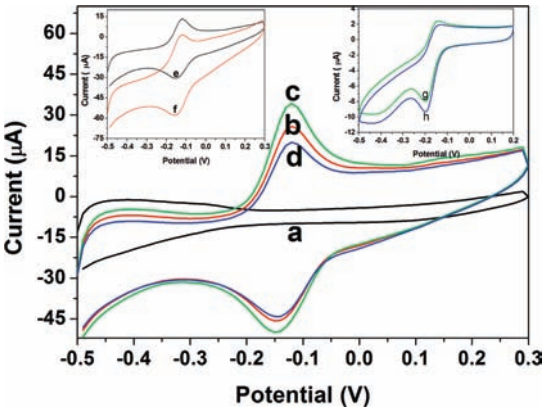


**Figure 2.** Cyclic voltammograms of (**a**) SPCE, (**b**) thionine/SPCE, (**c**) nanogold/thionine/SPCE, and (**d**) *anti*-SEB/nanogold/thionine/SPCE in pH 5.5 ABS. (Insets: electrochemical behaviors of the immunosensor toward 5.0 ng/mL SEB using (**e**, **f**) *anti*-SEB-HRPSiCNTs and (**g**, **h**) *anti*-SEB-CNTs as detection antibodies in pH 5.5 ABS, respectively. Notes: in pH 5.5 ABS (**e**, **g**) without and (**f**, **h**) with 8.0 mM $H_2O_2$.)

pH 5.5 ABS. No peak was observed for the bare SPCE (**Figure 2a**). When thionine was electropolymerized on the surface of SPCE, a couple of redox peaks, −150 mV and −120 mV, were obtained (**Figure 2b**), indicating that the immobilized thionine could act as a good electron mediator for electron transfer. The redox peak could be enhanced when the nanogold particles were assembled onto the surface of the thionine/SPCE (**Figure 2c**). The result suggested that gold nanoparticles favored the electron transfer. When *anti*-SEB antibodies were immobilized onto the surface of nanogold particles, however, the redox peak currents were decreased (**Figure 2d**).

To further verify the feasibility of the sandwich-type electrochemical immunoassay, the immunosensor was used for detection of 5.0 ng/mL SEB (as an example). The formed sandwich-type immunocomplex was investigated in pH 5.5 ABS before and after the addition of $H_2O_2$. As seen in **Figure 2e**,**f**, an obvious redox reaction appeared with a distinct increase of the reduction

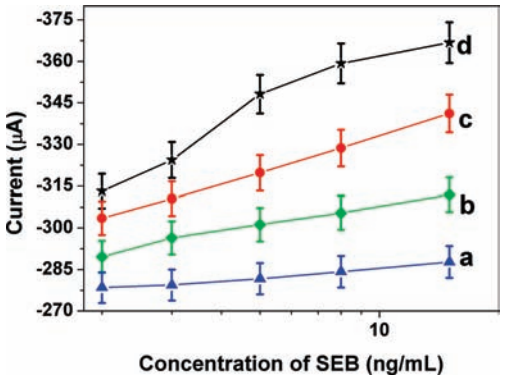


**Figure 3.** Comparison of electrochemical responses of the immunoassay using various detection antibodies toward different concentrations of SEB: (**a**) *anti*-SEB, (**b**) *anti*-SEB-CNT, (**c**) HRP-*anti*-SEB, and (**d**) *anti*-SEB-HRPSiCNT.

current and a decrease of the oxidation current upon the addition of $H_2O_2$ in pH 5.5 ABS. The catalytic current mainly derived from the immobilized HRP toward the reduction of $H_2O_2$ relative to the thionine−PBS system. Thus, we might quantitatively evaluate the concentration of SEB according to the relationship between the reduction current and SEB level. For comparison, the electrochemical behavior of the immunosensor using *anti*-SEB-CNTs as detection antibodies was studied in the absence and presence of $H_2O_2$. As indicated in **Figure 2g**,**h**, *anti*-SEB-CNT could slightly catalyze the reduction of $H_2O_2$.

**HRPSiCNTs for Signal Amplification.** To further clarify the amplified properties of the electrochemical immunoassay using the synthesized HRPSiCNTs, four detection antibodies including *anti*-SEB, HRP-*anti*-SEB, *anti*-SEB-CNT and *anti*-SEB-HRPSiCNT were utilized for the detection of five SEB standards with various concentrations. These immunoassay protocols are schematically illustrated in **Scheme 1b**. As indicated in **Figure 3a**,**b**, the use of CNT could obviously enhance the signal of the electrochemical immunoassay. The reason might be the fact that the coated CNTs could catalyze the reduction of $H_2O_2$ to some extent (*41*, *42*). Moreover, the signal could further increase using *anti*-SEB-HRPSiCNTs as detection antibodies (**Figure 3d**). In contrast to those of using HRP-*anti*-SEB (**Figure 3c**), the sensitivity using *anti*-SEB-HRPSiCNT could be greatly improved. The reason might be the fact that the catalytic currents not only derived from the doped HRP but also originated from the coated CNTs.

**Optimization of Experimental Conditions.** As seen in **Figure 3**, the amplification of the electrochemical signal is mainly derived from the doped HRP in the CNTs. To achieve a maximum HRP for each CNT, and avoid the leakage of the doped HRP from the CNTs, the ratio of HRP and TEOS should be optimized. Various volume ratios of HRP (100 mg/mL) and TEOS (98%, w/w) including 4:1, 3:1, 2:1, 1:1, 1:2, 1:3, and 1:4 (v/v) were used for the preparation of the HRPSiCNTs, which were employed for detection of 5.0 ng/mL SEB. As indicated in **Figure 4a**, the optimal current response was obtained at the volume ratio of 1:3. Thus, 1:3 of volume ratio of HRP and TEOS was selected for the preparation of HRPSiCNTs.

Incubation time and incubation temperature for the antigen−antibody interaction often affect the electrochemical responses of the immunoassay. To ensure the practical application of the immunoassay for real samples, a universal environment, such as room temperature, is preferable. Thus, all experiments were performed at RT (25 ± 1.0 °C) in this study. At this temperature, we investigated the effect of the incubation time on the current

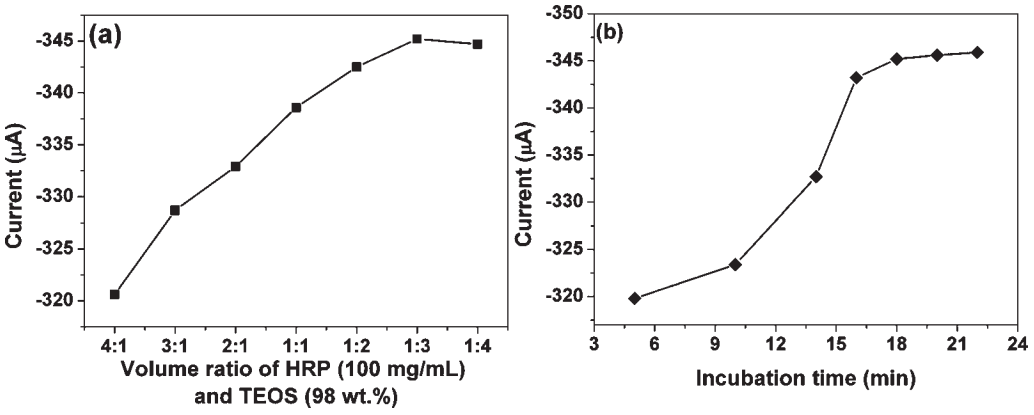


**Figure 4.** Effects of (**a**) volume ratio of HRP (100 mg/mL) and TEOS (98 wt %) for the preparation of HRPSiCNTs, and (**b**) incubation time for the antigen−antibody reaction on the electrochemical responses of the immunoassay (note: 5.0 ng/mL SEB as an example).

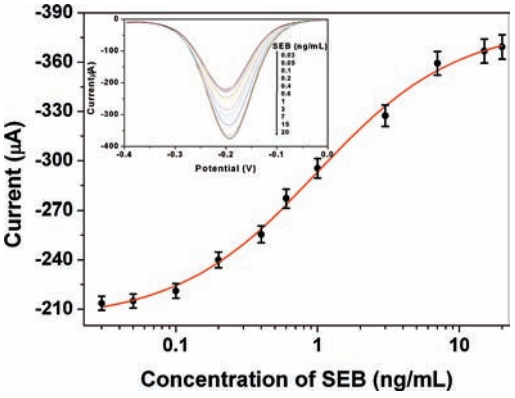


**Figure 5.** Calibration curves of the electrochemical immunoassays toward spiking SEB standards into blank fresh milk.

response of the immunoassay. As shown in **Figure 4b**, the current increased with the increasing incubation time, and trended to level off after 18 min. Longer incubation time could not improve the response. Therefore, 18 min of incubation time was used for detection of SEB.

**Analytical Performance.** The sensitive and dynamic range of the sandwich-type electrochemical immunoassay for the spiked SEB standards into fresh milk matrix was first assessed using *anti*-SEB-HRPSiCNTs as tracer and $H_2O_2$ as enzyme substrates under optimal conditions. A sigmoid regression curve between the reduction currents and the SEB concentration was obtained (**Figure 5**). The reduction current increased with the increase of the SEB concentration. As shown in the inset of **Figure 5**, the increase of reduction currents was linear in the range of 0.05 to 15 ng/mL SEB and the linear regression equation was adjusted to $i_{pc}$ ($\mu$A) = 292.6 + 29.5 × log$C_{[SEB]}$ (ng/mL) with a detection limit (LOD) of 10 pg/mL at a signal-to-noise ratio of 3$\sigma$ (where $\sigma$ is the standard deviation of the blank, $n$ = 15) ($R^2$ = 0.985). The precision of the electrochemical immunoassay was evaluated by calculating the intra- and interbatch variation coefficients (CVs, $n$ = 6). Experimental results suggested that the CVs of the assays using *anti*-SEB-HRPSiCNTs from the same batch were 8.3%, 7.6%, 6.8%, and 5.7% at the 0.08, 1.0, 5.0, and 12.0 ng/mL SEB levels, respectively, while the CVs of the assays using *anti*-SEB-HRPSiCNTs from different batches were 6.3%, 8.7%, 9.7%, and 5.2% at the above-mentioned analyte concentrations. Moreover, the *anti*-SEB-HRPSiCNTs displayed good stability. Analyzed from experimental data, as much as 90% of the initial current response was preserved after storage of the *anti*-SEB-HRPSiCNTs in pH 7.4 PBS for 23 days.

**Regeneration and Selectivity.** Regeneration of immunosensors is of interest for practical application. Although the antigen−antibody linkage can be broken under drastic conditions, the immobilized immunoproteins can also suffer from functional damage or even be released from the immunosorbents. As seen from our previous reports and experimental results (*23*, *24*, *43*−*45*), 0.1 M glycine-HCl (pH 2.8) could be used for the regeneration of the electrochemical immunosensor. After each immunoassay run, the immunosensor was regenerated by immersing into the glycine-HCl solution for 5 min and washing with pH 7.4 PBS, and then the following run cycle was carried out.

To investigate the differences in response of the immunoassay to interference degree of crossing recognition level, aflatoxin $B_1$ ($AFB_1$), aflatoxin $B_2$ ($AFB_2$), staphylococcal enterotoxin A (SEA), staphylococcal enterotoxin C (SEC), and interleukin-6 (IL-6) with various concentrations were injected into the detection system, respectively. The current responses to each type of analyte were recorded, and the results are listed in **Table 1**. As shown in **Table 1**, almost no response was observed toward $AFB_1$, $AFB_2$ and IL-6 while there is a high cross-reactivity with SEA and SEC. The reason might be the fact that the primary antibodies and secondary antibodies exhibited high cross reactivity with SEA and SEC of SEB similar structure. Thus, the selectivity of the electrochemical immunoassay is acceptable.

**Evaluation of Real Samples and Intralaboratory Validation.** The trueness and applicability of the electrochemical immunoassay for testing real food samples, namely, SEB spiked samples, including watermelon juice, soymilk, apple juice, and pork food, were assessed by using the electrochemical immunoassay and commercially available ELISA as a reference method. The experimental results are summarized in **Table 2**. The recovery in spiked samples is 94.5−116% for the electrochemical immunoassay. The regression equation for the experimental results obtained from two methods is $y = (0.96 \pm 0.13)x - (0.22 \pm 1.7)$ (ng/mL, $R^2$ = 0.987; $x$, SEB levels; $y$, reference values). The correlation between the two methods was investigated using $t$-tests for comparison of the experimental values of the intercept and slope to the ideal situation of zero intercept and slope of 1. These data were very close to the regression line, and the slope was close to 1, thereby revealing a good agreement between both analytical methods.

In conclusion, this manuscript describes the development and validation of a sandwich-type amplified electrochemical immunoassay of the detection of SEB (as a model analyte) in foodstuffs using carbon nanotubes (CNT) as carriers for the HRP reporter enzyme. The highlight of this study is to combine the nanocatalytic properties of carbon nanotubes with bioelectrocatalytic

**Table 1.** Interference Degree or Crossing Recognition Level of the Electrochemical Immunoassay

| | $C_{[interfering\ agents]}$ (ng/mL); detectable concentration[a] | | | | | | |
|---|---|---|---|---|---|---|---|
| crossing reagents[b] | 0 | 0.5 | 2 | 5 | 10 | mean ± SD | RSD (%) |
| SEB + $AFB_1$ | 5.0 | 5.04 ± 0.01 | 5.12 ± 0.13 | 5.34 ± 0.24 | 5.39 ± 0.56 | 5.18 ± 0.16 | 3.1 |
| SEB + $AFB_2$ | 5.0 | 5.03 ± 0.03 | 5.37 ± 0.56 | 5.67 ± 0.87 | 5.34 ± 0.64 | 5.28 ± 0.25 | 4.7 |
| SEB + SEA | 5.0 | 5.12 ± 0.02 | 5.97 ± 0.98 | 8.23 ± 0.76 | 13.56 ± 0.46 | 7.58 ± 3.21 | 42.3 |
| SEB + SEC | 5.0 | 5.18 ± 0.01 | 6.02 ± 0.23 | 8.43 ± 0.41 | 13.97 ± 0.25 | 7.72 ± 3.36 | 43.5 |
| SEB + IL-6 | 5.0 | 5.11 ± 0.04 | 5.34 ± 0.88 | 5.67 ± 0.52 | 5.89 ± 0.39 | 5.41 ± 0.34 | 6.2 |

[a] The average value of three assays, and the concentrations were calculated according the calibration curve. [b] Containing 5 ng/mL SEB and various concentrations of interfering agents.

**Table 2.** Comparison of Experimental Results for Determination of SEB in Real Food Samples as Obtained by the Electrochemical Immunoassay and ELISA as Reference Method

| | | | methods (mean ± SD, ng/mL)[a] and recovery (%) | |
|---|---|---|---|---|
| food sample | sample no. | dose of the spiked SEB (ng/mL) | electrochemical immunoassay | ELISA |
| watermelon juice | 1[b] | 0 | 0.09 ± 0.01 (−) | −[c] |
| | 2 | 1.2 | 1.32 ± 0.27 (110%) | 1.45 ± 0.16 (120%) |
| | 3 | 3.0 | 3.45 ± 0.49 (115%) | 3.21 ± 0.27 (107%) |
| | 4 | 7.0 | 6.78 ± 0.78 (96.9%) | 6.34 ± 0.29 (90.6%) |
| soymilk | 5[b] | 0 | 0.07 ± 0.01 (−) | − |
| | 6 | 2.5 | 2.65 ± 0.43 (106%) | 2.98 ± 0.11 (119%) |
| | 7 | 5.0 | 4.78 ± 0.29 (95.6%) | 5.02 ± 0.76 (100%) |
| | 8 | 9.0 | 8.98 ± 0.73 (99.8%) | 9.34 ± 0.98 (104%) |
| apple juice | 9[b] | 0 | − | − |
| | 10 | 1.5 | 1.46 ± 0.21 (97.3%) | 1.65 ± 0.27 (110%) |
| | 11 | 4.5 | 4.54 ± 0.98 (101%) | 4.89 ± 0.65 (109%) |
| | 12 | 9.0 | 9.76 ± 1.01 (108%) | 9.21 ± 0.46 (102%) |
| pork food | 13[b] | 0 | 0.08 ± 0.01 (−) | − |
| | 14 | 2.0 | 1.89 ± 0.24 (94.5%) | 2.01 ± 0.34 (101%) |
| | 15 | 5.0 | 5.78 ± 0.67 (116%) | 5.13 ± 0.81 (103%) |
| | 16 | 9.0 | 8.94 ± 0.24 (99.3%) | 8.91 ± 0.24 (99%) |

[a] Each sample was assayed in triplicate. [b] Without spiking SEB samples. [c] Not detected.

amplification of bioactive enzyme. Experimental results indicated that the electrochemical immunoassay exhibited high sensitivity, acceptable reproducibility and stability. Importantly, the electrochemical immunoassays can be further extended for detection of other low-concentration toxins in food by controlling the target antibody. We might suspect that such immunoassay approaches will evolve toward a very promising future for reliable point-of-care diagnostics of biocompounds, and as tools for intraoperation pathological testing, proteomics, and system biology.

## LITERATURE CITED


(1) Johnson, B.; Delehanty, J.; Lin, B.; Ligler, F. Immobilized praanthocyanidins for the capture of bacterial lipopolysaccharides. *Anal. Chem.* **2008**, *80*, 2113−2117.

(2) Delehanty, J.; Ligler, F. A microarray immunoassay for simultaneous detection of proteins and bacteria. *Anal. Chem.* **2002**, *74*, 5681−5687.

(3) Ricci, F.; Volpe, G.; Micheli, L.; Palleschi, G. A review on novel developments and applications of immunosensors in food analysis. *Anal. Chim. Acta* **2007**, *605*, 111−129.

(4) Oliveira, A.; Silva, L.; Andrade, P.; Valentao, P.; Guedes de Pinho, P. Determination of low molecular weight volatiles in *Ficus carica* using HS-SPME and GC/FID. *Food Chem.* **2010**, *121*, 1289−1295.

(5) Buchbauer, G.; Jirovetz, L.; Wasicky, M.; Nikiforov, A. Comparative investigation of douglas fir headspace samples, essential oils, and extracts (needles and twigs) using GC-FID and GC-FTIR-MS. *J. Agric. Food Chem.* **1994**, *42*, 2852−2854.

(6) Draper, W.; Ling, J.; Fowler, M.; Kharrazi, M.; Flessel, F.; Perera, S. Testing for persistent organic pollutants in banked maternal serum specimens. *ACS Symp. Ser.* **2007**, *951*, 49−69.

(7) Erk, T.; Bergmann, H.; Richling, E. A novel method for the quantification of quinic acid in food using stable isotope dilution analysis. *J. AOAC Int.* **2009**, *92*, 730−733.

(8) Aoki, Y.; Kotani, A.; Miyazawa, N.; Uchida, K.; Igarashi, Y.; Hirayama, N.; Hakamata, H.; Kusu, F. Determination of ethoxyquin by high-performance liquid chromatography with fluorescence detection and its application to the survey of residues in food products of animal origin. *J. AOAC Int.* **2010**, *93*, 277−283.

(9) Guillarme, D.; Schappler, J.; Rudaz, S.; Veuthey, J. Coupling ultra-high pressure liquid chromatography with mass spectrometry. *TrAC, Trends Anal. Chem.* **2010**, *29*, 15−27.

(10) Kanuer, M.; Ivleva, N.; Liu, X.; Niessner, R.; Haisch, C. Surface-enhanced raman scattering-based label-free microarray readout for the detection of microorganisms. *Anal. Chem.* **2010**, *82*, 2766−2772.

(11) Kupstat, A.; Knopp, D.; Niessner, R.; Kumke, M. Novel intramolecular energy transfer probe for the detection of Benzo[a]pyrene metabolites in a homogeneous competitive fluorescence immunoassay. *J. Phys. Chem. B* **2010**, *114*, 1666−1673.

(12) Tang, D.; Sauceda, J.; Lin, Z.; Ott, S.; Basova, E.; Goryacheva, I.; Biselli, S.; Niessner, R.; Knopp, D. Magnetic nanogold microspheres-based lateral flow immunodipstick for rapid detection of aflatoxin $B_2$ in food. *Biosens. Bioelectron.* **2009**, *25*, 514−518.

(13) Erickson, J.; Ligler, F. Analytical chemistry: Home diagnostics to music. *Nature* **2008**, *456*, 178−179.

(14) Taitt, C.; Anderson, G.; Lingerfelt, B.; Feldstein, M.; Ligler, F. Nine-analyte detection using an array-based biosensor. *Anal. Chem.* **2002**, *74*, 6114−6120.

(15) Tang, D. P.; Zhong, Z.; Niessner, R.; Knopp, D. Multifunctional magnetic beads-based electrochemical immunoassay for the detection of aflatoxin $B_1$ in food. *Analyst* **2009**, *134*, 1554−1560.

(16) Liebana, S.; Lermo, A.; Campoy, S.; Cortes, M.; Alegret, S.; Pividori, M. Rapid detection of Salmonella in milk by electrochemical magneto-immunosensing. *Biosens. Bioelectron.* **2009**, *25*, 510−513.

(17) Pividori, M.; Lermo, A.; Bonanni, A.; Alegret, S.; del Valle, M. Electrochemical immunosensor for the diagnosis of celiac disease. *Anal. Biochem.* **2009**, *388*, 229−234.

(18) Lai, G.; Yan, F.; Ju, H. Dual signal amplification of glucose oxidase-functionalized nanocomposites as trace label for ultrasensitive simultaneous multiplexed electrochemical detection of tumor markers. *Anal. Chem.* **2009**, *81*, 9730−9736.

(19) Xiang, Y.; Zhang, Y.; Chang, Y.; Chai, Y.; Wang, J.; Yuan, R. Reverse-micelle synthesis of electrochemically encoded quantum dot barcodes: application to electronic coding of a cancer marker. *Anal. Chem.* **2010**, *82*, 1138−1141.

(20) Zhang, J.; Lei, J.; Xu, C.; Ding, L.; Ju, H. Carbon nanohorns sensitized electrochemical immunosensor for rapid detection of microcystin-LR. *Anal. Chem.* **2010**, *82*, 1117−1122.

(21) Wu, Z.; Zhou, H.; Zhang, S.; Shen, G.; Yu, R. Electrochemical aptameric recognition system for a sensitive protein assay based on specific target binding-induced rolling circle amplification. *Anal. Chem.* **2010**, *82*, 2282−2289.

(22) Li, Y.; Cox, J.; Zhang, B. Electrochemical responses and electrocatalysis at single Au nanoparticles. *J. Am. Chem. Soc.* **2010**, *132*, 3047−3054.

(23) Tang, D.; Su, B.; Tang, J.; Ren, J.; Chen, G. Nanoparticles-Based Sandwich Electrochemical Immunoassay for Carbohydrate Antigen 125 with Signal Enhancement Using Enzyme-Coated Nanometer-Sized Enzyme-Doped Silica Beads. *Anal. Chem.* **2010**, *82*, 1527−1534.
(24) Tang, D.; Ren, J. In situ amplified electrochemical immunoassay for carcinoembryonic antigen using horseradish peroxidase-encapsulated nanogold hollow microspheres as labels. *Anal. Chem.* **2008**, *80*, 8064−8070.
(25) Liebana, S.; Lermo, A.; Campoy, S.; Barbe, J.; Alegret, S.; Pividori, M. Magneto immunoseparation of pathogenic bacteria and electrochemical magneto genosensing of the double-tagged amplicon. *Anal. Chem.* **2009**, *81*, 5812−5820.
(26) Yang, W.; Ratinac, K.; Ringer, S.; Thordarson, P.; Gooding, J.; Braet, F. Carbon nanomaterials in biosensors: should you use nanotubes or graphene? *Angew. Chem., Int. Ed.* **2010**, *49*, 2114−2138.
(27) Kauffman, D.; Sorescu, D.; Schofield, D.; Allen, B.; Jordan, K.; Star, A. Understanding the sensor response of metal-decorated carbon nanotubes. *Nano Lett.* **2010**, *10*, 958−963.
(28) Kauffman, D.; Star, A. Carbon nanotube gas and vapor sensors. *Angew. Chem., Int. Ed.* **2008**, *47*, 6550−6570.
(29) Nie, H.; Liu, S.; Yu, R.; Jiang, J. Phospholipid-coated carbon nanotubes as sensitive electrochemical labels with controlled-assembly-mediated signal transduction for magnetic separation immunoassay. *Angew. Chem., Int. Ed.* **2009**, *48*, 9862−9866.
(30) Wang, J.; Liu, G.; Jan, M. Ultrasensitive electrical biosensing of proteins and DNA: carbon-nanotube derived amplification of the recognition and transduction events. *J. Am. Chem. Soc.* **2004**, *126*, 3010−3011.
(31) Sadana, A.; Sadana, N. Toxins and pollutants detection on biosensor surface. *Handb. Biosens. Biosens. Kinet.* **2011**, 389−422.
(32) Savransky, V.; Pinelis, D.; Korolev, S.; Ionin, B.; Fegeding, K. Immunogenicity of the histidine-to-tyrosine staphylococcal enterotoxin B mutant protein in C3H/HeJ mice. *Toxicon* **2004**, *43*, 433−438.
(33) Kull, S.; Pauly, D.; Stormann, B.; Kirchner, S.; Stammler, M.; Dorner, M.; Lasch, P.; Dorner, B. Multiplex detection of microbial and plant toxins by immunoaffinity enrichment and matrix-assisted laser desorption/ionization mass spectrometry. *Anal. Chem.* **2010**, *82*, 2916−2924.
(34) Kim, J.; Anderson, G.; Erickson, J.; Golden, J.; Nasir, M.; Ligler, G. Multiplexed detection of bacteria and toxins using a microflow cytometer. *Anal. Chem.* **2009**, *81*, 5426−5432.
(35) Soto, C.; Martin, B.; Sapsford, K.; Blum, A.; Ratna, B. Toward single molecule detection of staphylococcal enterotoxin B: mobile sandwich immunoassay on gliding microtubules. *Anal. Chem.* **2008**, *80*, 5433−5440.
(36) Tang, D.; Yuan, R.; Chai, Y.; Zhang, L.; Zhong, X.; Dai, J.; Liu, Y. New amperometric and potentiometric immunosensors based on gold nanoparticles/tris(2,2′-bipyridyl)cobalt(III) multilayer films for hepatitis B surface antigen determinations. *Biosens. Bioelectron.* **2005**, *21*, 539−548.
(37) Yu, X.; Munge, B.; Patel, V.; Jensen, G.; Bhirde, A.; Gong, J.; Kim, S.; Gillespie, J.; Gutkind, J.; Papadimitrakopoulos, F.; Rusling, J. Carbon nanotube amplification strategies for highly sensitive immunodetection of cancer biomarkers. *J. Am. Chem. Soc.* **2006**, *128*, 11199−11205.
(38) Williams, K.; Veenhuizen, T.; De la Torre, B.; Eritja, R.; Dekker, C. Carbon Nanotubes with DNA recognition. *Nature* **2002**, *420*, 761−761.
(39) Baker, S.; Cai, W.; Lasseter, T.; Weidkamp, K.; Hamers, R. Covalently bonded adducts of deoxyribonucleic acid (DNA) oligonucleotides with single-wall carbon nanotubes: synthesis and hybridization. *Nano Lett.* **2002**, *2*, 1413−1417.
(40) Ren, J.; Tang, D.; Su, B.; Tang, J.; Chen, G. Glucose oxidase-doped magnetic silica nanostructures as labels for localized signal amplification of electrochemical immunosensors. *Nanoscale* **2010**, *2*, 1244−1249.
(41) Tasis, D.; Tagmatarchis, N.; Bianco, A.; Prato, M. Chemistry of carbon nanotubes. *Chem. Rev.* **2006**, *106*, 1105−1136.
(42) Bertoncello, P.; Forster, R. Nanostructured materials for electrochemiluminescence (ECL)-based detection methods: Recent advances and future perspectives. *Biosens. Bioelectron.* **2009**, *24*, 3191−3200.
(43) Tang, D.; Tang, J.; Su, B.; Ren, J.; Chen, G. Simultaneous determination of five-type hepatitis virus antigens in five minutes using an integrated automatic electrochemical immunosensor array. *Biosens. Bioelectron.* **2010**, *25*, 1658−1662.
(44) Tang, D.; Niessner, R.; Knopp, D. Flow-injection electrochemical immunosensor for the detection of human IgG based on glucose oxidase-derivated biomimetic interface. *Biosens. Bioelectron.* **2009**, *24*, 2125−2130.
(45) Tang, D.; Yuan, R.; Chai, Y. Ultrasensitive electrochemical immunosensor for clinical immunoassay using thionine-doped magnetic gold nanospheres as labels and horseradish peroxidase as enhancer. *Anal. Chem.* **2008**, *80*, 1582−1588.

**Received for review June 16, 2010. Revised manuscript received September 10, 2010. Accepted September 13, 2010. This work was jointly supported by the National Basic Research Program of China (2010CB732403), the NSFC (21075019, 20877019, and 20735002), the special project of Ministry of Health, China (200902009), the Key NSF of Fujian Province (D0520001), the Key Program of Science and Technology Department of Fujian Province, China (2007Y0026), NTU-MOE Academic Research Funds (RG65/08), and the High-Qualified Talent Funding of Fuzhou University (XRC-0929).**